Heliyon 10 (2024) e29304

Contents lists available at ScienceDirect

Heliyon

journal homepage: www.cell.com/heliyon

Research article

# Locating-dominating number of certain infinite families of convex polytopes with applications

Sakander Hayat [a,*], Naqiuddin Kartolo [a], Asad Khan [b,*], Mohammed J.F. Alenazi [c]

[a] *Mathematical Sciences, Faculty of Science, Universiti Brunei Darussalam, Jln Tungku Link, Gadong BE1410, Brunei Darussalam*
[b] *Metaverse Research Institute, School of Computer Science and Cyber Engineering, Guangzhou University, Guangzhou, Guangdong, 510006, PR China*
[c] *Department of Computer Engineering, College of Computer and Information Sciences (CCIS), King Saud University, Riyadh 11451, Saudi Arabia*

A R T I C L E I N F O

*MSC:*
05C69
90C05
05C10
92E10

*Keywords:*
Graph
Domination number
Locating-dominating number
Convex polytope
ILP model
Structure-property modeling

A B S T R A C T

A convex hull of finitely many points in the Euclidean space $\mathbb{R}^d$ is known as a convex polytope. Graphically, they are planar graphs i.e. embeddable on $\mathbb{R}^2$. Minimum dominating sets possess diverse applications in computer science and engineering. Locating-dominating sets are a natural extension of dominating sets. Studying minimizing locating-dominating sets of convex polytopes reveal interesting distance-dominating related topological properties of these geometrical planar graphs. In this paper, exact value of the locating-dominating number is shown for one infinite family of convex polytopes. Moreover, tight upper bounds on $\gamma_{l-d}$ are shown for two more infinite families. Tightness in the upper bounds is shown by employing an updated integer linear programming (ILP) model for the locating-dominating number $\gamma_{l-d}$ of a fixed graph. Results are explained with help of some examples. The second part of the paper solves an open problem in Khan (2023) [28] which asks to find a domination-related parameter which delivers a correlation coefficient of $\rho > 0.9967$ with the total $\pi$-electronic energy of lower benzenoid hydrocarbons. We show that the locating-dominating number $\gamma_{l-d}$ delivers such a strong prediction potential. The paper is concluded with putting forward some open problems in this area.

## 1. Introduction

Let us consider the undirected connected simple graph $\Gamma$. The set of vertices and edges in $\Gamma = (V, E)$ are $V$ and $E$, respectively. The *closed neighborhood* of a vertex $a \in V$ is $N_\Gamma[a] = \{b \in V \mid (b, a) \in E\} \cup \{a\}$, while the *open neighborhood* of a vertex a $V$ is $N_\Gamma(a) = \{b \in V \mid (b, a) \in E\}$. A dominating set in a graph $\Gamma = (V, E)$ is defined as a subset $D$ of $V$ (i.e., $D \subseteq V$) that satisfies the condition that the closed neighborhoods of all vertices in $D$ together encompass the entire set of vertices (i.e., $V$). Mathematically, this can be expressed $\cup_{a\in D} N[a] = V$. For example, for every vertex $a \in V \setminus D$, $N(a) \cap D \neq \emptyset$ implies that any such $a$ has minimum of one neighbors in $D$. The smallest multiplicity of such a dominating set in $\Gamma$ is known as the domination number $\gamma(\Gamma)$ of $\Gamma$.

Another way to approach the concept of a dominating set is to assign a weight of 1 to each vertex in $D$ and a weight of 0 to vertices in $V \setminus D$. In this situation, if $|N[a] \cap D| \geq 1$ for each $a \in V$ and the sum of weights for closed neighborhoods is not less than 1, then $D$ is a dominating set of $\Gamma$, we denote a dominating set by $S$. If, for all distinct vertices $a, b \in V \setminus S$, it holds that

* Corresponding authors.
*E-mail addresses:* sakander1566@gmail.com (S. Hayat), naqi342@gmail.com (N. Kartolo), asad@gzhu.edu.cn (A. Khan), mjalenazi@ksu.edu.sa (M.J.F. Alenazi).

https://doi.org/10.1016/j.heliyon.2024.e29304
Received 24 October 2023; Received in revised form 27 March 2024; Accepted 4 April 2024

Available online 9 April 2024
2405-8440/

$N(b) \cap S \neq N(a) \cap S$, then the dominating set $S \subseteq V$ is called a *locating-dominating set* (see Hernando et al. [1]). The minimum cardinality of a locating-dominating set is denoted by $\gamma_{l-d}(\Gamma)$, which stands for the *locating-dominating number* of $\Gamma$.

According to the following theorem, the locating-dominating number on regular graphs has a tight lower bound.

We give the following important result by Slater [2]:

**Theorem 1.1.** [2] *For a $k$-regular graph $\Gamma$ on $V$ vertices, we have*

$$\gamma_{l-d}(\Gamma) \geq \left\lceil \frac{2 \cdot v}{k+3} \right\rceil.$$

Bača introduced graphs of convex polytopes [3]. In the articles [4], [5], [6], and [7], various convex polytopes, including $Q_n$, $R_n$, $D_n$, $S_n$, $T_n$, and $U_n$, have been studied for a variety of properties. Specifically, [5] and [6] revealed that the metric dimension of $U_n$, $S_n$, $R_n$, $T_n$, and $Q_n$ are equal to 3, while [7] explored minimizing doubly-resolving sets and strong resolvability of $D_n$ and $T_n$. In addition, Salman et al. [8] analyzed three optimization problems including the strong metric, fault-tolerant as well as the local metric dimension problems and applied them to $U_n$ and $S_n$ families of convex polytopes. Next, due to Simić et al. [9], we present an updated integer linear programming model for the locating-dominating number of graphs.

## 2. Integer linear programming (ILP) model for $\gamma_{l-d}$

In [10], the minimum identifying code problem using integer linear programming (ILP) formulation was provided. Decision variables $z_\ell$ are defined as follows for $S$ to be an identifying set:

$$z_\ell = \begin{cases} 1, & \ell \in S \\ 0, & \ell \notin S \end{cases} \tag{2.1}$$

The minimum identifying code problem from [10] is therefore stated with its ILP formulation as follows:

$$\min \sum_{\ell \in V} z_\ell \tag{2.2}$$

subject to

$$\sum_{p \in N[\ell]} x_p \geq 1, \qquad \ell \in V \tag{2.3}$$

$$\sum_{p \in N[\ell] \nabla N[q]} x_p \geq 1 \quad \ell, q \in V,\ \ell \neq q \tag{2.4}$$

$$z_\ell \in \{0, 1\}, \qquad \ell \in V \tag{2.5}$$

In order to ensure that the identifying code set has a minimum cardinality, the aim function in Equation (2.2) and constraints in Equation (2.3) define $S$ as a dominating set. Constraints in Equation (2.4) indicate an identifying characteristic, whereas constraints from Equation (2.5) describe the binary nature of the decision variables $z_\ell$.

The locating-dominating problem cannot be solved directly using this formulation. As a result, it has to be modified by switching constraints from Equation (2.4) to Equation (2.6).

$$z_\ell + x_q + \sum_{p \in N[\ell] \nabla N[q]} x_p \geq 1 \quad \ell, q \in V, \ell \neq q \tag{2.6}$$

Here $\nabla$ is the symmetric difference operator between two sets. When vertices $\ell$ and $q$ are not neighbors, constraints in Equation (2.4) and Equation (2.6) are the same, for example, $N[\ell] \nabla N[q] = \{\ell, p\} \cup (N(\ell) \nabla N(q))$. The change between Equation (2.4) and Equation (2.6) takes effect if vertices $\ell$ and $q$ are adjacent to one another, which implies that $\ell \in N(q)$. As a result, $S$ must contain some $p \in N(\ell) \nabla N(q)$ or not less than 1 of the vertices $\ell$, $q$, according to constraint in Equation (2.6). Constraints in Equation (2.6) and Equation (2.4) are similar since $N[q] \nabla N[\ell] = \{\ell, p\} \cup (N(q) \nabla N(\ell))$ when $q, \ell$, $\ell \nsim q$ are not neighbors.

It was said in [11] that if $d(b, a) \geq 3$, then $b, a$ do not have any neighbors in common, hence it is not necessary to examine whether $N(b) \cap S \neq N(a) \cap S$ are equivalent. As a result, we may reduce the number of constraints the locating requirement generates which is computationally significant for larger graphs.

This concept would help further to improve constraints in Equation (2.6):

$$z_\ell + x_q + \sum_{p \in N[\ell] \nabla N[q]} x_p \geq 1 \quad \ell, q \in V, \ell \neq q, d(\ell, q) \leq 2 \tag{2.7}$$

For problems of small dimensions, the exact optimal value can determine with the use of the suggested formulation with lesser constraints. Furthermore, as demonstrated by [12], effective metaheuristic methods can be used to produce unsatisfactory solutions for large dimensions.

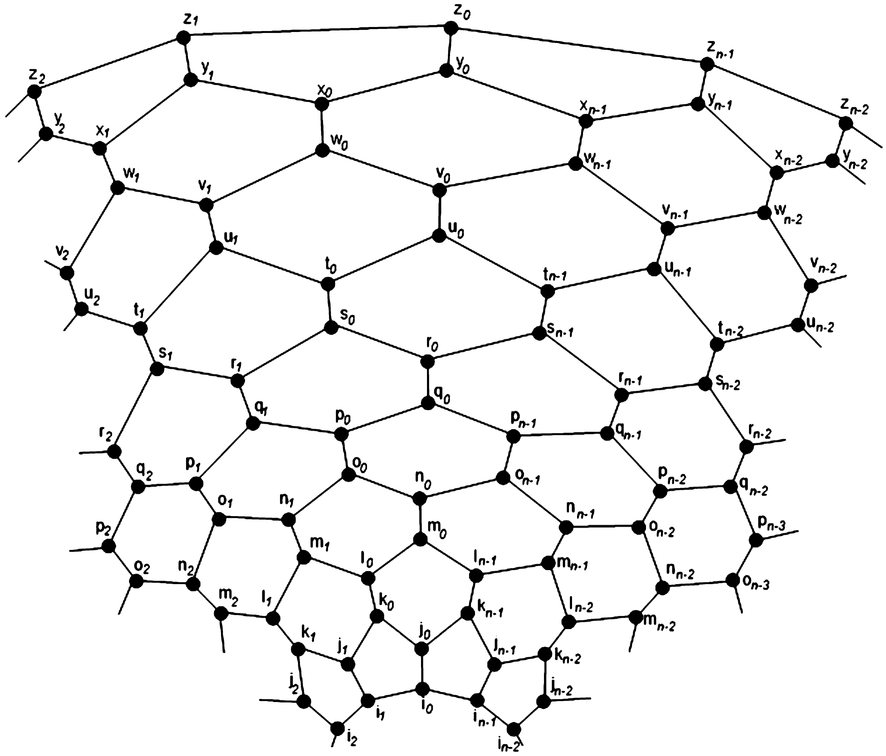


**Fig. 1.** Graphical structure of the $n$-dimensional of $T_n$ convex polytope.

## 3. Exact values for $\gamma_{l-d}$

### 3.1. Convex polytope $T_n$

In [13], Fig. 1 displays the graph of the convex polytope $T_n$. The set of vertices of $T_n$ are $V(T_n) = \{i_\ell, j_\ell, k_\ell, l_\ell, m_\ell, n_\ell, o_i, p_\ell, q_\ell, r_\ell, s_\ell, t_\ell, u_\ell, v_\ell, w_\ell, z_\ell, y_\ell, z_\ell \mid \ell = 0, \dots, n-1\}$ and the set of edges are $E(T_n) = \{(i_\ell, i_{\ell+1}), (i_\ell, j_\ell), (j_\ell, k_\ell), (j_{\ell+1}, k_1), (k_\ell, l_\ell), (l_\ell, m_\ell), (m_\ell, n_\ell), (l_{\ell+1}, m_\ell), (n_{\ell+1}, o_\ell), (n_\ell, o_\ell), (p_\ell, q_\ell), (o_\ell, p_\ell), (p_{\ell+1}, q_\ell), (r_\ell, s_\ell), (q_\ell, r_\ell), (r_{\ell+1}, s_\ell), (t_\ell, u_\ell), (s_\ell, t_\ell), (t_{\ell+1}, u_\ell), (v_\ell, w_\ell), (u_\ell, v_\ell), (v_{\ell+1}, w_\ell), (w_\ell, z_\ell), (z_\ell, y_\ell), (x_{\ell+1}, y_\ell), (y_\ell, z_\ell)(z_\ell, z_{\ell+1})\}$.

Let $F_n(\Gamma)$ be the number of $n$-gonal faces in the graph $\Gamma$. Then, in $T_n$, we have $F_n(T_n) = 2$, $F_5(T_n) = 2n$ and $F_6(T_n) = 7n$. Note that the family of $T_n$ is related to the family of carbon nanocones [14,15].

**Theorem 3.1.** *For $T_n$ such that $n \geq 4$, we have*

$$\gamma_{l-d}(T_n) = 6n.$$

**Proof.** Note that $T_n$ is 3-regular with $|V(T_n)| = 18n$. It is demonstrated that

$$\gamma_{l-d}(T_n) \geq \left\lceil \frac{2 \cdot 18n}{3+3} \right\rceil = 6n$$

by Theorem 1.1. Now show that the locating-dominating set of $T_n$, the set $S$, defined as $S = \{j_\ell, m_\ell, p_\ell, s_\ell, v_\ell, y_\ell \mid \ell = 0, \dots, n-1\}$. The intersections of set $S$ with the neighborhoods $N[a]$, or $S \cap N[a]$, are all distinct and non-empty, as illustrated in Table 1. As, $S$ represents a locating dominating set of $T_n$ with $|S| = 6n$, we can conclude that $\gamma_{l-d}(T_n) \leq 6n$. Moreover, it has been previously established that $\gamma_{l-d}(T_n) \geq 6n$. Therefore, it follows that $\gamma_{l-d}(T_n) = 6n$. $\square$

Next, Theorem 3.1 is elaborated by an example. For this example, we consider 6-dimensional $T_n$, i.e., $T_6$. See Fig. 2 for a depiction of $T_6$.

**Example 1.** Note that $T_6$ is 3-regular and thus by Theorem 1.1, we have $\gamma_{l-d}(T_6) \geq 30$. In order to show $\gamma_{l-d}(T_6) \leq 30$, we consider the set $S = \{j_\ell, m_\ell, p_\ell, s_\ell, v_\ell, y_\ell \mid \ell = 0, \dots, 5\}$. Note that $|S| = 30$. We show that $S$ forms a locating-dominating set. For $0 \leq \ell \leq 5$, the intersections are

**Table 1**
Locating-dominating vertices in $T_n$.

| $a \in V \setminus S$ | $S \cap N[a]$ | $a \in V \setminus S$ | $S \cap N[a]$ |
|---|---|---|---|
| $i_\ell$ | $\{j_\ell\}$ | $k_\ell$ | $\{j_\ell, j_{\ell+1}\}$ |
| $l_\ell$ | $\{m_\ell, m_{\ell+1}\}$ | $n_\ell$ | $\{m_\ell\}$ |
| $o_\ell$ | $\{p_\ell\}$ | $q_\ell$ | $\{p_\ell, p_{\ell+1}\}$ |
| $r_\ell$ | $\{s_\ell, s_{\ell+1}\}$ | $t_\ell$ | $\{s_\ell\}$ |
| $u_\ell$ | $\{v_\ell\}$ | $w_\ell$ | $\{v_\ell, v_{\ell+1}\}$ |
| $x_\ell$ | $\{y_\ell, y_{\ell+1}\}$ | $z_\ell$ | $\{y_\ell\}$ |

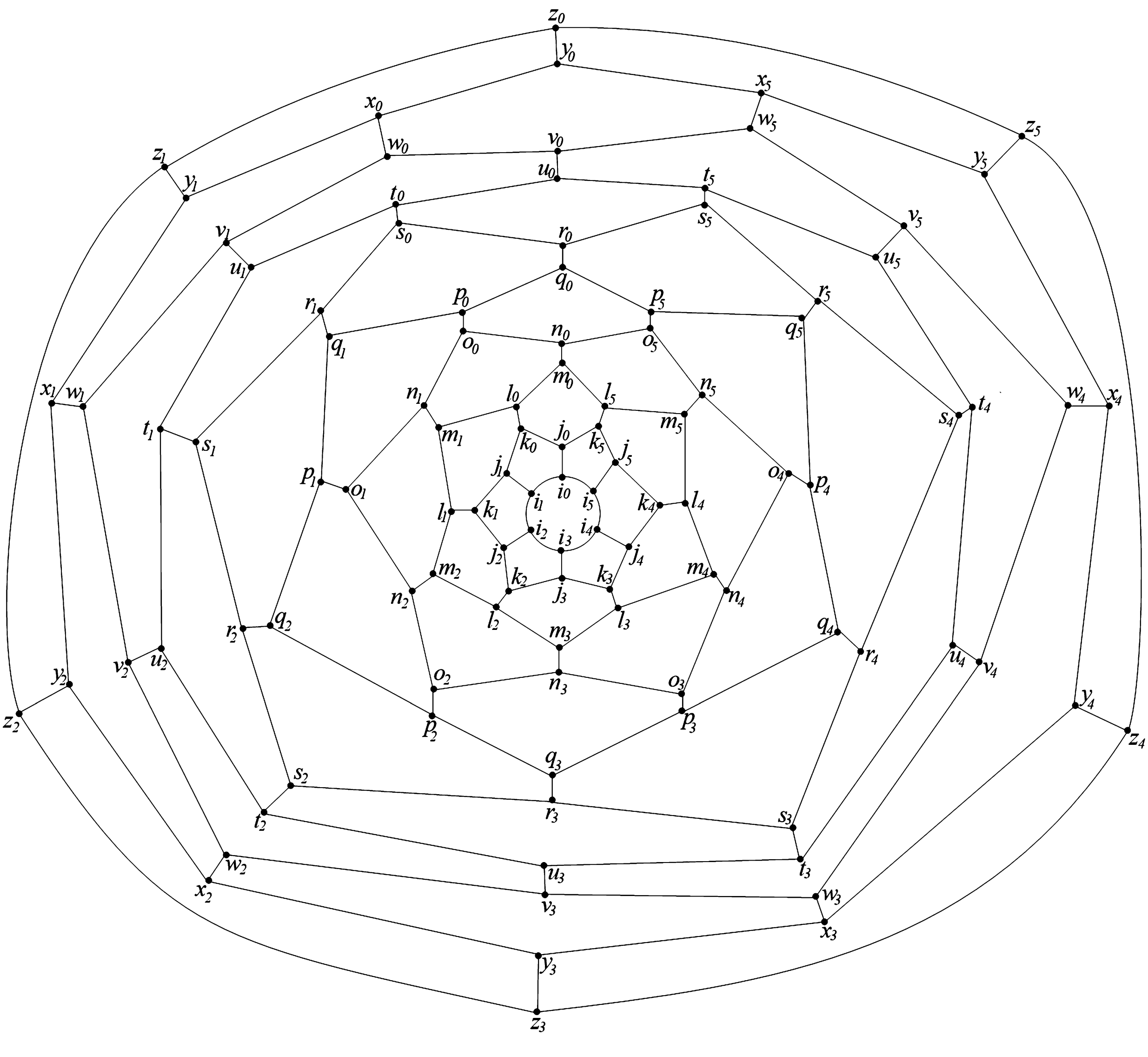


**Fig. 2.** Graphical structure of $T_6$.

$$S \cap N[i_\ell] = \{j_\ell\},\ S \cap N[k_\ell] = \{j_\ell, j_{\ell+1}\},\ S \cap N[l_\ell] = \{m_\ell, m_{\ell+1}\},\ S \cap N[n_\ell] = \{m_\ell\},$$

$$S \cap N[o_\ell] = \{p_\ell\}, S \cap N[q_\ell] = \{p_\ell, p_{\ell+1}\},\ S \cap N[r_\ell] = \{s_\ell, s_{\ell+1}\},\ S \cap N[t_\ell] = \{s_\ell\},$$

$$S \cap N[z_\ell] = \{y_\ell\},\ S \cap N[u_\ell] = \{v_\ell\}, S \cap N[w_\ell] = \{v_\ell, v_{\ell+1}\},\ S \cap N[x_\ell] = \{y_\ell, y_{\ell+1}\}.$$

The non-empty distinctive nature of all these intersections implies that $S$ forms a locating-dominating set. Thus, $\gamma_{l-d}(T_6) \leq 30$ implying $\gamma_{l-d}(T_6) = 30$. This conclusion is in agreement with Theorem 3.1.

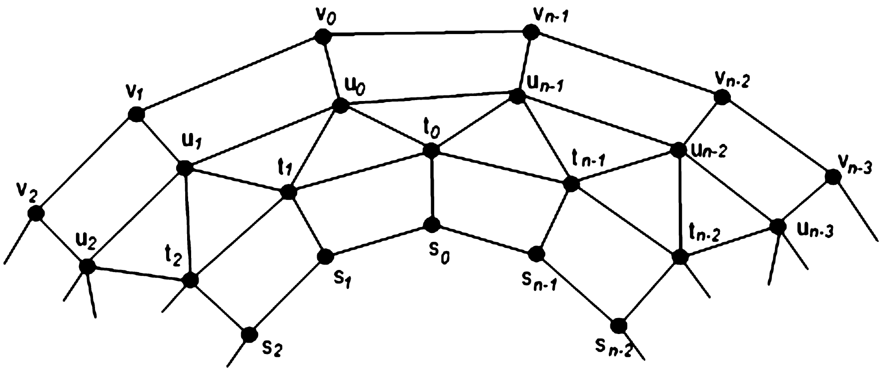


**Fig. 3.** Graphical structure of the $n$-dimensional of $N_n$ convex polytope.

Next, we present some upper bounds on the locating-dominating number $\gamma_{l-d}$ of two other important families of convex polytopes.

## 4. Tight upper bounds for $\gamma_{l-d}$

Let us first consider the family $N_n$.

### 4.1. Convex polytope $N_n$

In [9], Fig. 3 presents the graphical structure of $N_n$. The set of vertices of $N_n$ are $V(N_n) = \{s_\ell, t_\ell, u_\ell, v_\ell | \ell = 0, 1, \ldots, n-1\}$ and the set of edges are $E(N_n) = \{(s_\ell, s_{\ell+1}), (s_\ell, t_\ell), (t_\ell, t_{\ell+1}), (t_\ell, u_i), (t_{\ell+1}, u_\ell), (u_\ell, v_\ell), (v_\ell, v_{\ell+1})\}$.

Note that $N_n$ has $F_4(N_n) = 2n$ and $F_3(N_n) = 2n$.

**Theorem 4.1.**

$$\gamma_{l-d}(N_n) \leq \left\lceil \frac{4 \cdot n}{3} \right\rceil.$$

**Proof.** The polytope $N_n$ has $4n$ vertices and has two distinct degrees i.e., 3 & 5. Let

$$S = \begin{cases} \{t_{3\ell}, v_{3\ell+2}, u_{3\ell+1}, s_{3\ell+1} | \ell = 0, \ldots, p-1\}, & n \equiv 0(\mod 3), n = 3p \\ \{t_{3\ell}, v_{3\ell}, u_{3\ell+1}, s_{3\ell+2} | \ell = 0, \ldots, p-1\}\} \cup \{v_{3p}, t_{3p}\}, & n \equiv 1(\mod 3), n = 3p+1 \\ \{s_{3\ell}, t_{3\ell+1}, u_{3\ell+2}, v_{3\ell} | \ell = 0, \ldots, p-1\} \cup \{v_{3p}, s_{3p}, t_{3p+1}\}, & n \equiv 2(\mod 3), n = 3p+2 \end{cases}$$

Let us now show that vertices in $S$ are locating-dominating for $N_n$. Consider three potential cases in order to do that:

Table 3 illustrates that set $S$ have intersections with the neighborhoods of all vertices in the complement of set $S$ (represented as $V \setminus S$) that are both distinct and non-empty.

*Case 1*: $n = 3p$. Table 3 illustrates that the neighborhoods of all vertices in the complement of the set $S$ (represented as $V \setminus S$) have intersections with $S$ that are both distinctive and non-empty. Some of the intersection formulas used in the neighborhoods of vertices in the complement of set $S$ may appear to be similar, they are in fact distinct from each other. For example, $N[t_{3\ell+1}] \cap S = \{s_{3\ell+1}\} \neq \{s_{3(\ell+1)}\} = N[s_{3\ell+2}] \cap S$. This is due to the fact that the indices used in the intersection formulas are different, resulting in different sets where $3(\ell+1) = 3\ell + 3 \neq 3\ell + 1$. Similarly to $N[v_{3\ell+2}] \cap S = \{u_{3\ell+2}, v_{3(\ell+1)}\} \neq \{u_{3\ell+2}, v_{3\ell}\} = N[v_{3\ell+1}] \cap S$, although there may be some common elements in these intersections, they are distinct sets with their own unique elements.

*Case 2*: $n = 3p+1$. Similar to the earlier possibility, the intersections of the set $S$ with all neighborhoods $N[a]$, represented as $S \cap N[a]$, are distinct and non-empty. This fact is also depicted in Tables 2 & 3.

*Case 3*: $n = 3p+2$. Similar to both earlier possibilities, the intersections of the set $S$ with all neighborhoods $N[a]$, represented as $S \cap N[a]$, are distinct and non-empty, also depicted in Tables 2 & 3. □

**Remark 1.** Next, we show that the upper bound in Theorem 4.1 is tight as follows: CPLEX solver has been employed by utilizing the ILP formulation possessing inequalities/constraints in Equation (2.1), Equation (2.2), Equation (2.3) & Equation (2.7), optimal solutions for the $\gamma_{l-d}(N_n)$ have been derived as follows: $\gamma_{l-d}(N_5) = 7$, $\gamma_{l-d}(N_6) = 8$, $\gamma_{l-d}(N_7) = 10, \ldots, \gamma_{l-d}(N_{15}) = 20, \ldots, \gamma_{l-d}(N_{50}) = 67$. Thus, it turns out that, the bound in Theorem 4.1 is tight.

Take note that $Q_n$ have the same set $S$ with $N_n$. For convex polytopes $N_n$ (Fig. 3), it only has $n$ extra edges $(u_\ell, u_{\ell+1})$, $\ell = 0, \ldots, n-1$ compared to $Q_n$ (Fig. 4). Therefore, as depicted in Table 3, intersections of $S$ with vertices' neighborhoods in $V \setminus S$ are all similar with the addition of vertices $(u_\ell, u_{\ell+1})$, $\ell = 0, \ldots, n-1$. Table 2 present additional data for $N_n$.

**Table 2**
Additional data compared to $Q_n$ for $N_n$.

| $n$ | $a \in V \setminus S$ | $S \cap N[a]$ | $a \in V \setminus S$ | $S \cap N[a]$ |
|---|---|---|---|---|
| $3p$ | $u_{3\ell}$ | $\{u_{3\ell+1}, t_{3\ell}\}$ | $u_{3\ell+2}$ | $\{t_{3(\ell+1)}, u_{3\ell+1}, v_{3(\ell+2)}\}$ |
| $3p+1$ | $u_{3\ell}$ | $\{u_{3\ell+1}, t_{3\ell}, v_{3\ell}\}$ | $u_{3\ell+2}$ | $\{u_{3\ell+1}, t_{3(\ell+1)}\}$ |
| $3p+2$ | $u_{3\ell}$ | $\{u_{3\ell-1}, v_{3\ell}, t_{3\ell+1}\}$ | $u_{3\ell+1}$ | $\{t_{3\ell+1}, u_{3\ell+2}\}$ |
| | $u_{3p}$ | $\{t_{3p+1}, u_{3p-1}, v_{3p}\}$ | | |

**Table 3**
Locating-dominating vertices in $Q_n$.

| $n$ | $a \in V \setminus S$ | $S \cap N[a]$ | $a \in V \setminus S$ | $S \cap N[a]$ |
|---|---|---|---|---|
| $3p$ | $s_{3\ell}$ | $\{s_{3\ell+1}, t_{3\ell}\}$ | $s_{3\ell+2}$ | $\{s_{3\ell+1}\}$ |
| | $t_{3\ell+1}$ | $\{s_{3\ell+1}, t_{3\ell}, u_{3\ell+1}\}$ | $t_{3\ell+2}$ | $\{t_{3(\ell+1)}, u_{3\ell+1}\}$ |
| | $u_{3\ell}$ | $\{t_{3\ell}\}$ | $u_{3\ell+2}$ | $\{t_{3(\ell+1)}, v_{3(\ell+2)}\}$ |
| | $v_{3\ell}$ | $\{v_{3(\ell-1+2)}\}$ | $v_{3\ell+1}$ | $\{u_{3(\ell+1)}, v_{3\ell+2}, u_{3\ell+1}\}$ |
| $3p+1$ | $s_{3\ell}$ | $\{s_{3(\ell-1)+2}, t_{3\ell}\}$ | $s_{3\ell+1}$ | $\{s_{3\ell+2}\}$ |
| | $t_{3\ell+1}$ | $\{t_{3\ell}, u_{3\ell+1}\}$ | $t_{3\ell+2}$ | $\{s_{3\ell+2}, t_{3(\ell+1)}, u_{3\ell+1}\}$ |
| | $u_{3\ell}$ | $\{t_{3\ell}, v_{3\ell}\}$ | $u_{3\ell+2}$ | $\{t_{3(\ell+1)}\}$ |
| | $v_{3\ell+1}$ | $\{v_{3\ell+1}, v_{3\ell}\}$ | $v_{3\ell+2}$ | $\{v_{3(\ell+1)}\}$ |
| | $s_{3p}$ | $\{t_{3p}, s_{3(p-1)+2}\}$ | $u_{3p}$ | $\{t_0, t_{3p}, v_{3p}\}$ |
| | $s_0$ | $\{t_0\}$ | | |
| $3p+2$ | $s_{3\ell+1}$ | $\{s_{3\ell}, t_{3\ell+1}\}$ | $s_{3\ell+2}$ | $\{s_{3(\ell+1)}\}$ |
| | $t_{3\ell}$ | $\{s_{3\ell}, t_{3\ell+1}, u_{3(\ell-1)+2}\}$ | $t_{3\ell+2}$ | $\{t_{3i+1}, u_{3i+2}\}$ |
| | $u_{3\ell}$ | $\{t_{3\ell+1}, v_{3\ell}\}$ | $u_{3\ell+1}$ | $\{t_{3\ell+1}\}$ |
| | $v_{3\ell+1}$ | $\{v_{3\ell}\}$ | $v_{3\ell+2}$ | $\{u_{3\ell+2}, v_{3(\ell+1)}\}$ |
| | $t_{3p}$ | $\{s_{3p}, t_{3p}, u_{3(p-1)+2}\}$ | $u_{3p}$ | $\{t_{3p+1}, v_{3p}\}$ |
| | $s_{3p+1}$ | $\{s_{3p}, t_{3p+1}\}$ | $u_{3p+1}$ | $\{t_{3p+1}\}$ |
| | $v_{3p+1}$ | $\{v_{3p}\}$ | $t_0$ | $\{s_0, t_1, t_{3p+1}\}$ |

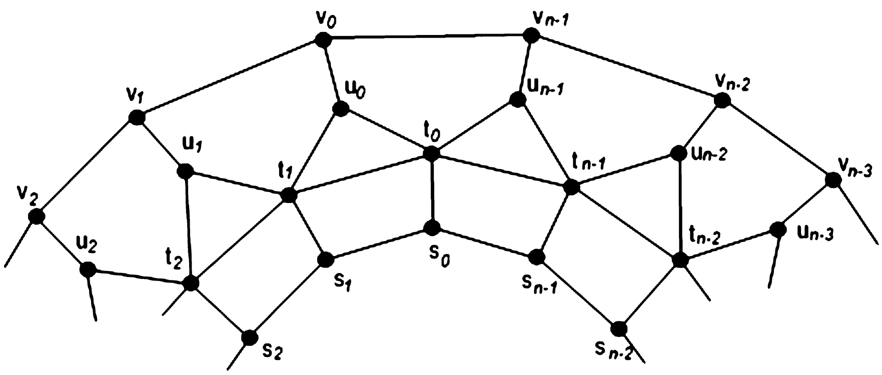


**Fig. 4.** Graphical structure of the $n$-dimensional of $Q_n$ convex polytope.

The information presented in both Table 2 and Table 3 indicates that, intersections of $S$ with the neighborhoods of every vertex in $V \setminus S$ are distinct and non-empty, based on all 3 cases. Thus $S$ is a locating-dominating set for both $Q_n$ and $N_n$. Therefore, $\gamma_{l-d}(N_n) \le \left\lceil \frac{4 \cdot n}{3} \right\rceil$, since

$$|S| = \left\lceil \frac{4 \cdot n}{3} \right\rceil.$$

Next, Theorem 4.1 is explained with the help of an example. For the example, we consider 7-dimensional $N_n$, i.e., $N_7$. See Fig. 5 for a depiction of $N_7$.

**Example 2.** We employ Theorem 4.1 to show that $\gamma_{l-d}(N_7) = 10$. We consider the set $S = \{a_2, a_5, b_0, b_3, b_6, c_1, c_4, d_0, d_3, d_6\}$. Note that $|S| = 10$. We show that $S$ forms a locating-dominating set. The intersections are

$$S \cap N[a_0] = \{b_0\},\ S \cap N[a_1] = \{a_2\},\ S \cap N[a_3] = \{a_2, b_3\},\ S \cap N[a_4] = \{a_5\},\ S \cap N[a_6] = \{a_5, b_6\},$$

$$S \cap N[b_1] = \{b_0, c_1\}\ , S \cap N[b_2] = \{a_2, b_3, c_1\},\ S \cap N[b_4] = \{b_3, c_4\},\ S \cap N[b_5] = \{a_5, b_6, c_4\},$$

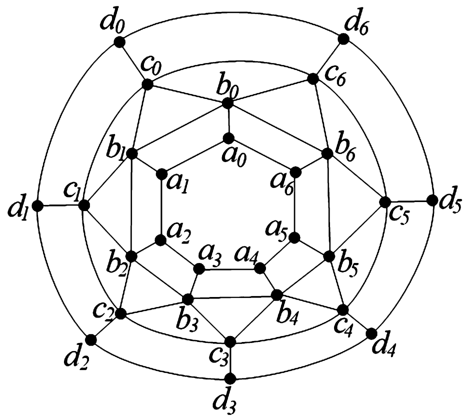


**Fig. 5.** Graphical structure of $N_7$.

$$S \cap N[c_0] = \{b_0, c_1, d_0\},\ S \cap N[c_2] = \{b_3, c_1\},\ S \cap N[c_3] = \{b_3, c_4, d_3\},\ S \cap N[c_5] = \{b_6, c_4\},$$
$$S \cap N[c_6] = \{b_0, b_6, d_6\},\ S \cap N[d_1] = \{c_1, d_0\},\ S \cap N[d_2] = \{d_3\},\ S \cap N[d_4] = \{c_4, d_3\},$$
$$S \cap N[d_5] = \{d_6\}.$$

The non-empty distinctive nature of all these intersections implies that $S$ forms a locating-dominating set. Thus, $\gamma_{l-d}(N_7) \leq 10$. CPLEX solver has been employed by utilizing the ILP formulation possessing constraints (2.1), (2.2), (2.3) & (2.7) to show that $\gamma_{l-d}(N_7) = 10$. This, in fact, is in agreement with Theorem 4.1.

### 4.2. Convex polytope $S_n$

In [9] Fig. 7 showcased the graphical structure of $S_n$. The set of vertices of $S_n$ are $V(S_n) = \{s_\ell, t_\ell, u_\ell, v_\ell, w_\ell | \ell = 0, 1, \ldots, n-1\}$ and the set of edges are $E(S_n) = \{(s_\ell, s_{\ell+1}), (s_\ell, t_\ell), (t_\ell, t_{\ell+1}), (t_\ell, u_\ell), (u_\ell, u_{\ell+1})(u_\ell, v_\ell), (u_{\ell+1}, v_\ell), (v_\ell, w_{\ell+1})\}$.

For $S_n$, notice that we have $F_4(N_n) = 2n$, $F_5(N_n) = n$ and $F_3(N_n) = n$.

**Theorem 4.2.**

$$\gamma_{l-d}(S_n) \leq \left\lceil \frac{5 \cdot n}{3} \right\rceil.$$

**Proof.** Let

$$S = \begin{cases} \{t_{3\ell}, s_{3\ell+1}, u_{3\ell+1}, w_{3\ell}, v_{3\ell+2} | \ell = 0, \ldots, p-1\}, & n \equiv 0 (\mod 3), n = 3p \\ \{s_{3p}, u_{3p}, w_{3p}\} \cup \{s_{3\ell}, t_{3\ell+2}, u_{3\ell}, v_{3\ell+1}, w_{3\ell} | \ell = 0, \ldots, p-1\}, & n \equiv 1 (\mod 3), n = 3p+1 \\ \{s_{3p+1}, t_{3p}, u_{3p+1}, w_{3p+1}\} & \\ \cup \{s_{3\ell+1}, w_{3\ell+1}, u_{3\ell+1}, t_{3\ell}, v_{3\ell+2} | \ell = 0, \ldots, p-1\}, & n \equiv 2 (\mod 3), n = 3p+2 \end{cases}$$

Next, we deliver that the vertices in $S$ form a locating-dominating set in $U_n$. We need to take into consideration three potential cases to achieve that, just as we did in the proofs of earlier theorems. In all three cases, Table 5 demonstrates that the vertices' neighborhoods in the complement of the set $S$ (represented as $V \setminus S$) have intersections with the set $S$ that are both distinct and non-empty.

Take note that $U_n$ have the same set $S$ with $S_n$. For convex polytopes $S_n$ (Fig. 7), it only has $n$ extra edges $(u_\ell, u_{\ell+1})$, $\ell = 0, \ldots, n-1$ compared to $U_n$ (Fig. 6). Therefore, as depicted in Table 3, intersections of $S$ with the neighborhoods of the vertices in $V \setminus S$ are all similar with the addition of vertices $(u_\ell, u_{\ell+1})$, $\ell = 0, \ldots, n-1$. Table 4 present additional data for $S_n$.

The information presented in both Table 4 and Table 5 indicates that, intersections of $S$ with the neighborhoods of every vertex in $V \setminus S$ are distinct and non-empty, based on all 3 cases. Thus $S$ is a locating-dominating set for both $U_n$ and $S_n$. Therefore, $\gamma_{l-d}(S_n) \leq \left\lceil \frac{5 \cdot n}{3} \right\rceil$, since

$$|S| = \left\lceil \frac{5 \cdot n}{3} \right\rceil. \quad \square$$

**Remark 2.** Next, we show that the upper bound in Theorem 4.2 is tight as follows: CPLEX solver has been employed by utilizing the ILP formulation possessing inequalities/constraints (2.1), (2.2), (2.3) & (2.7), optimal solutions for the $\gamma_{l-d}(S_n)$ have been derived

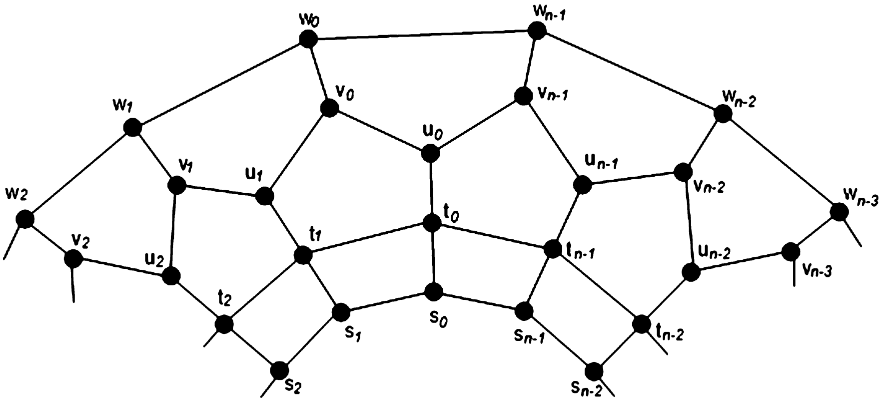


**Fig. 6.** Graphical structure of the $n$-dimensional of $U_n$ convex polytope.

**Table 4**
Additional data compared to $U_n$ for $S_n$.

| $n$ | $a \in V \setminus S$ | $S \cap N[a]$ | $a \in V \setminus S$ | $S \cap N[a]$ |
|---|---|---|---|---|
| $3p$ | $u_{3\ell}$ | $\{t_{3\ell}, v_{3(\ell-1)+2}, u_{3\ell+1}\}$ | $u_{3\ell+2}$ | $\{v_{3\ell+2}, u_{3\ell+1}\}$ |
| $3p+1$ | $u_{3\ell+1}$ | $\{v_{3\ell+1}, u_{3\ell}\}$ | $u_{3\ell+2}$ | $\{v_{3\ell+1}, t_{3\ell+2}, u_{3\ell+1}\}$ |
| $3p+2$ | $u_{3\ell}$ | $\{t_{3\ell}, u_{3\ell+1}, v_{3(\ell-1)+2}\}$ | $u_{3\ell+2}$ | $\{v_{3\ell+2}, u_{3\ell+1}\}$ |
| | $u_{3p}$ | $\{v_{3(p-1)+2}, u_{3p+1}, t_{3p}\}$ | $u_0$ | $\{t_0, u_1\}$ |

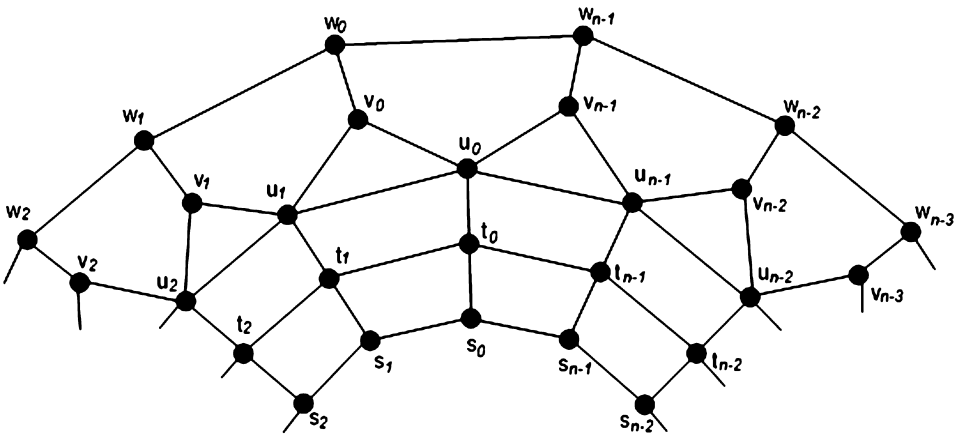


**Fig. 7.** Graphical structure of the $n$-dimensional of $S_n$ convex polytope.

as follows: $\gamma_{l-d}(S_5) = 9$, $\gamma_{l-d}(S_6) = 10$, $\gamma_{l-d}(S_7) = 12, \ldots, \gamma_{l-d}(S_{15}) = 25, \ldots, \gamma_{l-d}(S_{50}) = 84$. Thus, it turns out that, the bound in Theorem 4.2 is tight.

Next, Theorem 4.2 is explained with help of an example. For the example, we consider 6-dimensional $S_n$, i.e., $S_6$. See Fig. 8 for a depiction of $S_6$.

**Example 3.** We employ Theorem 4.2 to show that $\gamma_{l-d}(S_6) = 10$. We consider the set $S = \{a_1, a_4, b_0, b_3, c_1, c_4, d_2, d_5, e_0, e_3\}$. Note that $|S| = 10$. We show that $S$ forms a locating-dominating set. The intersections are

$$S \cap N[a_0] = \{a_1, b_0\},\ S \cap N[a_2] = \{a_1\},\ S \cap N[a_3] = \{a_4, b_3\},\ S \cap N[a_5] = \{a_4\},$$

$$S \cap N[b_1] = \{a_1, b_0, c_1\}, S \cap N[b_2] = \{b_3\},\ S \cap N[b_4] = \{a_4, b_3, c_4\}\ S \cap N[b_5] = \{b_0\},$$

$$S \cap N[c_0] = \{b_0, c_1, d_5\},\ S \cap N[c_2] = \{c_1, d_2\},\ S \cap N[c_3] = \{b_3, c_4, d_2\},\ S \cap N[c_5] = \{c_4, d_5\},$$

$$S \cap N[d_0] = \{c_1, e_0\},\ S \cap N[d_1] = \{e_1\}, S \cap N[d_3] = \{c_4, e_3\},\ S \cap N[d_4] = \{c_4\},\ S \cap N[e_1] = \{e_0\},$$

$$S \cap N[e_2] = \{d_2, e_3\},\ S \cap N[e_4] = \{e_3\}, S \cap N[e_5] = \{d_5, e_0\}.$$

**Table 5**
Locating-dominating vertices in $U_n$.

| $n$ | $a \in V \setminus S$ | $S \cap N[a]$ | $a \in V \setminus S$ | $S \cap N[a]$ |
|---|---|---|---|---|
| $3p$ | $s_{3\ell}$ | $\{s_{3\ell+1}, t_{3\ell}\}$ | $s_{3\ell+2}$ | $\{s_{3\ell+1}\}$ |
| | $t_{3\ell+1}$ | $\{s_{3\ell+1}, t_{3\ell}, u_{3\ell+1}\}$ | $t_{3\ell+2}$ | $\{t_{3(\ell+1)}, u_{3\ell+1}\}$ |
| | $u_{3\ell}$ | $\{t_{3\ell}, v_{3(\ell-1)+2}\}$ | $u_{3\ell+2}$ | $\{v_{3\ell+2}\}$ |
| | $v_{3\ell}$ | $\{u_{3\ell+1}, w_{3\ell}\}$ | $v_{3\ell+1}$ | $\{u_{3\ell+1}\}$ |
| | $w_{3\ell+1}$ | $\{w_{3\ell}\}$ | $w_{3\ell+2}$ | $\{v_{3\ell+2}, w_{3(\ell+1)}\}$ |
| $3p+1$ | $s_{3\ell+1}$ | $\{s_{3\ell}\}$ | $s_{3\ell+2}$ | $\{s_{3(\ell+1)}, t_{3\ell+2}\}$ |
| | $t_{3\ell}$ | $\{s_{3\ell}, u_{3\ell}, t_{3(\ell-1)+2}\}$ | $t_{3\ell+1}$ | $\{t_{3\ell+2}\}$ |
| | $u_{3\ell+1}$ | $\{v_{3\ell+1}\}$ | $u_{3\ell+2}$ | $\{t_{3\ell+2}, v_{3\ell+1}\}$ |
| | $v_{3\ell}$ | $\{u_{3\ell}, w_{3\ell}\}$ | $v_{3\ell+2}$ | $\{u_{3(\ell+1)}\}$ |
| | $w_{3\ell+1}$ | $\{v_{3\ell+1}, w_{3\ell}\}$ | $w_{3\ell+2}$ | $\{w_{3(\ell+1)}\}$ |
| | $t_{3p}$ | $\{s_{3p}, t_{3(p-1)+2}, u_{3p}\}$ | $v_{3p}$ | $\{u_{3p}, w_{3p}\}$ |
| | $t_0$ | $\{s_0, u_0\}$ | | |
| $3p+2$ | $s_{3\ell}$ | $\{s_{3\ell+1}, t_{3\ell}\}$ | $s_{3\ell+2}$ | $\{s_{3\ell+1}\}$ |
| | $t_{3\ell+1}$ | $\{s_{3\ell+1}, t_{3\ell}, u_{3\ell+1}\}$ | $t_{3\ell+2}$ | $\{t_{3(\ell+1)}\}$ |
| | $u_{3\ell}$ | $\{v_{3(\ell-1)+2}, t_{3\ell}\}$ | $u_{3\ell+2}$ | $\{v_{3\ell+2}\}$ |
| | $v_{3\ell}$ | $\{u_{3\ell+1}\}$ | $v_{3\ell+1}$ | $\{u_{3\ell+1}, e_{3\ell+1}\}$ |
| | $w_{3\ell}$ | $\{w_{3\ell+1}\}$ | $w_{3\ell+2}$ | $\{v_{3\ell+2}, w_{3\ell+1}\}$ |
| | $s_{3p}$ | $\{s_{3p+1}, t_{3p}\}$ | $u_{3p}$ | $\{t_{3p}, v_{3(p-1)+2}\}$ |
| | $v_{3p}$ | $\{u_{3p+1}\}$ | $w_{3p}$ | $\{w_{3p+1}\}$ |
| | $t_{3p+1}$ | $\{s_{3p+1}, t_0, t_{3p}, u_{3p+1}\}$ | $v_{3p+1}$ | $\{u_{3p+1}, w_{3p+1}\}$ |
| | $s_0$ | $\{s_1, s_{3p+1}, t_0\}$ | $u_0$ | $\{t_0\}$ |
| | $w_0$ | $\{w_1, w_{3p+1}\}$ | | |

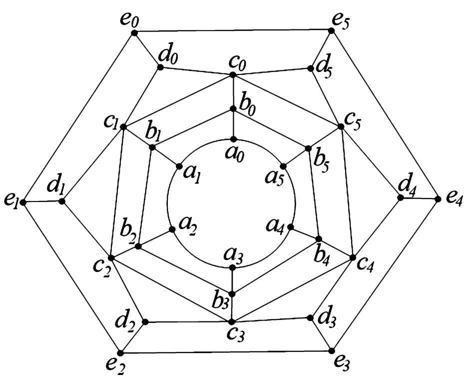


**Fig. 8.** Graphical structure of $S_6$.

The non-empty distinctive nature of all these intersections implies that $S$ forms a locating-dominating set. Thus, $\gamma_{l-d}(S_6) \le 10$. CPLEX solver has been employed by utilizing the ILP formulation possessing constraints (2.1), (2.2), (2.3) & (2.7) to show that $\gamma_{l-d}(S_6) = 10$. This shows that $\gamma_{l-d}(S_6) = 10$ and this is in agreement with Theorem 4.2.

## 5. Application of $\gamma_{l-d}$ in structure-property modeling

In this section, we study an important application of the locating-dominating number in structure-property modeling of benzene hydrocarbons.

Structure-property modeling of the total $\pi$-electronic energy ($E_\pi$) of benzenoid hydrocarbons (BHs) has been an active area of research recently. For instance, Lučić et al. [16] showed that the sum-connectivity and product-connectivity indices are closely interrelated to each other and they predict $E_\pi$ of BHs with significant accuracy. They chose lower 30 BHs for their study as test molecules. The work of Lučić et al. [16] was later extended to the generalized version of both sum/product connectivity indices i.e., $\chi_\alpha$ and $\chi_\alpha^s$ and derived the value(s) for which these indices give the best correlation with $E_\pi$ of BHs for lower 30 BHs. The study concluded that $\chi_{-0.2661}$ and $\chi^s_{-0.5601}$ deliver the best prediction $E_\pi$ of BHs. Hayat et al. [17] (resp. Hayat et al. [18]) studied the predictive potential of commonly occurring degree-based (resp. distance-based) for $E_\pi$ of BHs. For correlation ability of eigenvalues-based graphical indices in predicting $E_\pi$ of BHs, we refer the reader to [19] and [20]. For the importance of structure-property modeling, we refer the reader to [21–23]. Regarding some recent progress on structure-property modeling of physicochemical properties of nanostructures and bio-molecular networks, we refer to [24–27].

Recently, Khan [28] conducted a comparative study of seven domination-related parameters (*not including* $\gamma_{l-d}$) to correlate the $E_\pi$ of lower BHs. Out of those seven parameters, the study concluded that the paired domination number $\gamma_p$ delivers the best predictive ability with correlation coefficient $\rho = 0.9967$. The study was concluded with the following open problem:

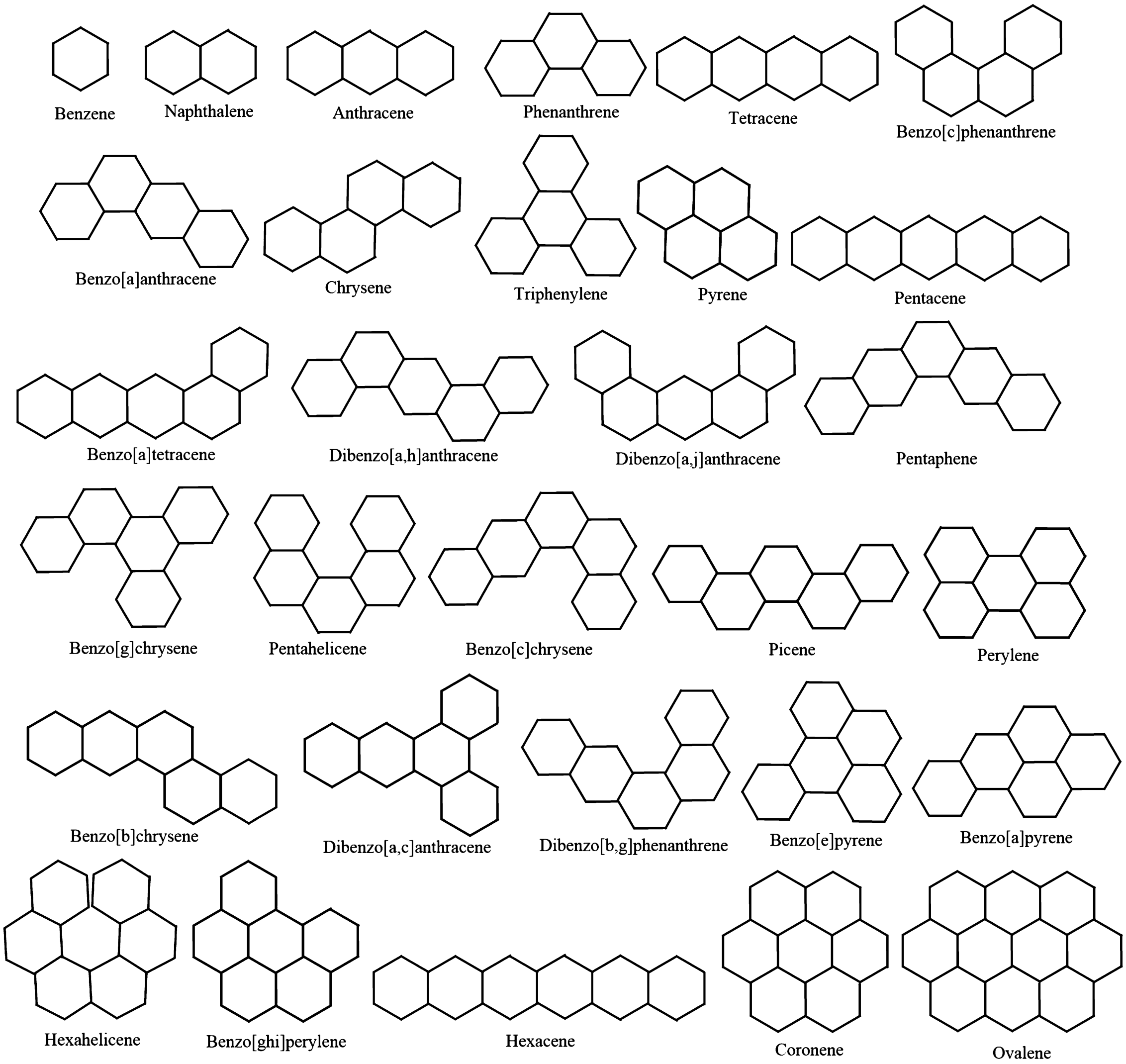


**Fig. 9.** Chemical graphs of the 30 test molecules considered for this study.

**Problem 1.** Does there exist a domination-related graphical parameter such that the correlation coefficient with $E_\pi$ of benzenoid hydrocarbons is $\rho > 0.9967$?

In this section, we answer Problem 1 and show that the locating-dominating number produces even stronger predictive potential with $E_\pi$ of BHs having correlation coefficient $\rho = 0.9987 > 0.9967$. In order to show it, we consider the lower 30 BHs as our test molecules. Fig. 9 exhibits the lower 30 BHs considered in this study.

Next, we compute the locating-dominating number $\gamma_{l-d}$ of the 30 BHs presented in Fig. 9. Table 6 delivers the locating-dominating number $\gamma_{l-d}$ and $E_\pi(\beta)$ measured in $\beta$ units for the 30 lower BHs showcased in Fig. 9. We used the data in Table 6 to conduct the detailed correlation & regression analysis. First, we calculate the correlation coefficient and it is $\rho = 0.9987$ which is significantly higher than the minimum threshold in Problem 1. Next, we conduct a detailed statistical analysis of the data. Our analysis suggested that most data-fitting regression model is, in fact, linear. The following are the linear regression model (with 95% confidence intervals for the slope & intercept), correlation coefficient $\rho$, the standard error of fit $s$, the determination coefficient $r^2$ for the data in Table 6.

$$E_\pi(\beta) = -1.003_{\pm 0.5066} + 2.911_{\pm 0.0490}\gamma_{l-d}, \qquad \rho = 0.9987,\ s = 0.3134,\ r^2 = 0.9981.$$

In what follows, we deliver the scatter plot between $\gamma_{l-d}$ and $E_\pi$ for 30 lower BHs. See Fig. 10.

## 6. Conclusion and future work

In this paper, we study the locating-dominating number of certain infinite families of convex polytopes. We find exact value of $\gamma_{l-d}$ for the infinite family $T_n$ and tight upper bounds on $\gamma_{l-d}$ are derived for two more infinite families that are $N_n$ and $S_n$.

**Table 6**
$E_\pi(\beta)$ and $\gamma_{l-d}$ values for 30 lower BHs (see Fig. 9).

| Molecule | $\gamma_{l-d}$ | $E_\pi(\beta)$ |
|---|---|---|
| Benzene | 3 | 8 |
| Naphthalene | 5 | 13.6832 |
| Anthracene | 7 | 19.3137 |
| Phenanthrene | 7 | 19.4483 |
| Tetracene | 9 | 24.9308 |
| Benzo[c]phenanthrene | 9 | 25.1875 |
| Benzo[a]anthracene | 9 | 25.1012 |
| Chrysene | 9 | 25.1922 |
| Triphenylene | 9 | 25.2745 |
| Pyrene | 9 | 22.5055 |
| Pentacene | 11 | 30.544 |
| Benzo[a]tetracene | 11 | 30.7255 |
| Dibenzo[a,h]anthracene | 11 | 30.8805 |
| Dibenzo[a,j]anthracene | 11 | 30.8795 |
| Pentaphene | 11 | 30.7627 |
| Benzo[g]chrysene | 11 | 30.999 |
| Pentahelicene | 11 | 30.9362 |
| Benzo[c]chrysene | 11 | 30.9386 |
| Picene | 11 | 30.9432 |
| Benzo[b]chrysene | 11 | 30.839 |
| Dibenzo[a,c]anthracene | 11 | 30.9418 |
| Dibenzo[b,g]phenanthrene | 11 | 30.8336 |
| Perylene | 10 | 28.2453 |
| Benzo[e]pyrene | 10 | 28.3361 |
| Benzo[a]pyrene | 10 | 28.222 |
| Hexahelicene | 13 | 36.6814 |
| Benzo[ghi]perylene | 11 | 31.4251 |
| Hexacene | 13 | 36.1557 |
| Coronene | 12 | 34.5718 |
| Ovalene | 16 | 46.4974 |

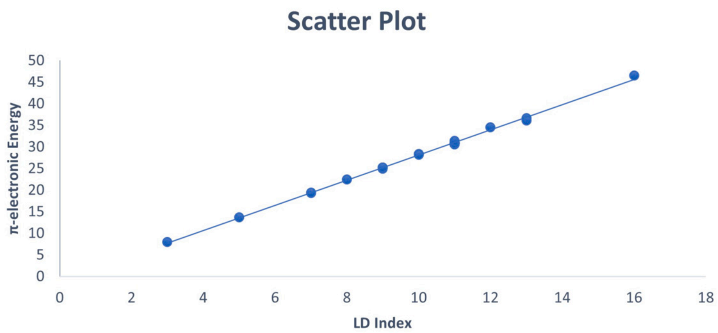


**Fig. 10.** Scatter plot for between $\gamma_{l-d}$ and $E_\pi$ for 30 lower BHs.

We employed an updated integer linear programming model in CPLEX solver to show tightness in the obtained upper bounds. We present an application of $\gamma_{l-d}$ in structure-property modeling of the total $\pi$-electronic energy of benzenoid hydrocarbons. This, in turn, answers positively to Problem 1 by Khan [28].

We propose the following open problems:

**Problem 2.** Find the exact values of $\gamma_{l-d}$ for both families of $n$-dimensional convex polytopes $N_n$ and $S_n$.

**Problem 3.** Find the exact value of $\gamma_{l-d}$ for the infinite families of triangular graphs & square grid graphs.

The quest for finding the most suitable domination-related parameter for predicting $E_\pi(\beta)$ is still ongoing. Thus, we have the following problem.

**Problem 4.** Does there exist a domination-related graphical parameter such that the correlation coefficient with $E_\pi$ of benzenoid hydrocarbons is $\rho > 0.9987$?

## Authors' contributions

All authors contributed equally to this work.


## Funding

S. Hayat is supported by UBD Faculty Research Grants (No. UBD/RSCH/1.4/FICBF(b)/2022/053). A. Khan was sponsored by the Key Laboratory of Philosophy and Social Sciences in Guangdong Province of Maritime Silk Road of Guangzhou University (GD22TWCXGC15) and the National Natural Science Foundation of China (Grant No. 622260-101). M.J.F. Alenazi extends his appreciation to Researcher Supporting Project number (RSPD2024R582), King Saud University, Riyadh, Saudi Arabia.


## CRediT authorship contribution statement

**Sakander Hayat:** Writing – review & editing, Writing – original draft, Software, Formal analysis, Conceptualization. **Naqiuddin Kartolo:** Writing – original draft, Validation, Methodology, Investigation, Formal analysis, Data curation. **Asad Khan:** Writing – review & editing, Visualization, Validation, Supervision, Project administration, Investigation, Data curation. **Mohammed J.F. Alenazi:** Writing – review & editing, Validation, Software, Resources, Funding acquisition.

## Declaration of competing interest

The authors declare that they have no known competing financial interests or personal relationships that could have appeared to influence the work reported in this paper.

## Data availability

No data was used for the research described in the article. No data associated with this study was deposited into a publicly available repository.


## Acknowledgements

The reviewers suggested significant improvement to the submitted version for which the authors are grateful.


## References


[1] C. Hernando, M. Mora, I.M. Pelayo, LD-graphs and global location-domination in bipartite graphs, Electron. Notes Discrete Math. 46 (2014) 225–232.
[2] P.J. Slater, Locating dominating sets and locating-dominating sets, in: Y. Alavi, A. Schwenk (Eds.), Graph Theory, Combinatorics, and Algorithms, vol. 2, Proceedings of the Seventh Quadrennial International Conference on the Theory and Applications of Graphs, Western Michigan University, John Wiley & Sons, New York, 1995, pp. 1073–1079.
[3] M. Bača, Labelings of two classes of convex polytopes, Util. Math. 34 (1988) 24–31.
[4] M. Bača, On magic labellings of convex polytopes, Ann. Discrete Math. 51 (1992) 13–16.
[5] M. Imran, A.Q. Baig, A. Ahmad, Families of plane graphs with constant metric dimension, Util. Math. 88 (2012) 43–57.
[6] M. Imran, S.A.U.H. Bokhary, A.Q. Baig, On families of convex polytopes with constant metric dimension, Comput. Math. Appl. 60 (2010) 2629–2638.
[7] J. Kratica, V. Kovačević-Vujčić, M. Č angalović, M. Stojanović, Minimal doubly resolving sets and the strong metric dimension of some convex polytopes, Appl. Math. Comput. 218 (2012) 9790–9801.
[8] M. Salman, I. Javaid, M.A. Chaudhry, Minimum fault-tolerant, local and strong metric dimension of graphs, arXiv:1409.2695 [math.CO], 2014.
[9] A. Simić, M. Bogdanović, J. Milošević, The binary locating-dominating number of some convex polytopes, Ars Math. Contemp. 13 (2) (2017) 367–377.
[10] N. Bousquet, A. Lagoutte, Z. Li, A. Parreau, S. Thomassé, Identifying codes in hereditary classes of graphs and VC-dimension, SIAM J. Discrete Math. 29 (2015) 2047–2064.
[11] D.B. Sweigart, J. Presnell, R. Kincaid, An integer program for open locating dominating sets and its results on the hexagon-triangle infinite grid and other graphs, in: 2014 Systems and Information Engineering Design Symposium (SIEDS), Charlottesville, Virginia, 2014, pp. 29–32.
[12] S. Hanafi, J. Lazić, N. Mladenović, I. Wilbaut, C. Crévits, New variable neighbourhood search based 0-1 MIP heuristics, Yugosl. J. Oper. Res. 25 (2015) 343–360.
[13] H. Raza, S. Hayat, X.-F. Pan, Binary locating-dominating sets in rotationally-symmetric convex polytopes, Symmetry 10 (12) (2018) 727.
[14] M. Arockiaraj, J. Clement, K. Balasubramanian, Topological properties of carbon nanocones, Polycycl. Arom. Compd. 40 (5) (2020) 1332–1346.
[15] S. Hayat, M. Imran, On topological properties of nanocones $CNC_k[n]$, Stud. Univ. Babes-Bolyai Chem. 59 (4) (2014) 113–128.
[16] B. Lučić, N. Trinajstić, B. Zhou, Comparison between the sum-connectivity index and product-connectivity index for benzenoid hydrocarbons, Chem. Phys. Lett. 475 (1–3) (2009) 146–148.
[17] S. Hayat, S. Khan, A. Khan, J.B. Liu, Valency-based molecular descriptors for measuring the $\pi$-electronic energy of lower polycyclic aromatic hydrocarbons, Polycycl. Arom. Compd. 42 (4) (2022) 1113–1129.
[18] S. Hayat, S. Khan, A. Khan, M. Imran, Distance-based topological descriptors for measuring the $\pi$-electronic energy of benzenoid hydrocarbons with applications to carbon nanotubes, Math. Methods Appl. Sci. (2020), https://doi.org/10.1002/mma.6668.
[19] M.Y.H. Malik, S. Hayat, S. Khan, A. Binyamin, Predictive potential of spectrum-based topological descriptors for measuring the $\pi$-electronic energy of benzenoid hydrocarbons with applications to boron triangular and boron $\alpha$-nanotubes, Math. Methods Appl. Sci. (2021), https://doi.org/10.1002/mma.7161.
[20] S. Hayat, S. Khan, A. Khan, M. Imran, A computer-based method to determine predictive potential of distance-spectral descriptors for measuring the $\pi$-electronic energy of benzenoid hydrocarbons with applications, IEEE Access 9 (2021) 19238–19253.
[21] M. Arockiaraj, A.B. Greeni, A.R.A. Kalaam, Linear versus cubic regression models for analyzing generalized reverse degree based topological indices of certain latest corona treatment drug molecules, Int. J. Quant. Chem. 123 (2023) e27136.

[22] M. Arockiaraj, D. Paul, J. Clement, S. Tigga, K. Jacob, K. Balasubramanian, Novel molecular hybrid geometric-harmonic-Zagreb degree based descriptors and their efficacy in QSPR studies of polycyclic aromatic hydrocarbons, SAR QSAR Environ. Res. 34 (7) (2023) 569–589.

[23] D. Paul, M. Arockiaraj, K. Jacob, J. Clement, Multiplicative versus scalar multiplicative degree based descriptors in QSAR/QSPR studies and their comparative analysis in entropy measures, Eur. Phys. J. Plus 138 (2023) 323.

[24] A. Ullah Aurangzeb, S. Zaman, A new perspective on the modeling and topological characterization of H-Naphtalenic nanosheets with applications, J. Mol. Model. 28 (2022) 211.

[25] A. Ullah Shamsudin, S. Zaman, A. Hamraz, Zagreb Connection topological descriptors and structural property of the triangular chain structures, Phys. Scr. 8 (2023) 025009.

[26] A. Ullah, S. Zaman, A. Hamraz, M. Muzammal, On the construction of some bioconjugate networks and their structural modeling via irregularity topological indices, Eur. Phys. J. E 46 (2023) 72.

[27] A. Ullah, S. Zaman, A. Hussain, A. Jabeen, M.B. Belay, Derivation of mathematical closed form expressions for certain irregular topological indices of 2D nanotubes, Sci. Rep. 13 (2023) 11187.

[28] S. Khan, Comparative study of domination parameters with the $\pi$-electronic energy of benzenoid hydrocarbons, Int. J. Quant. Chem. (2023), https://doi.org/10.1002/qua.27192.